2024 IEEE 27th International Conference on
Intelligent Transportation Systems (ITSC)
September 24- 27, 2024. Edmonton, Canada

Enhancing Large-Scale Evacuations of Electric Vehicles through Integration of Mobile Charging Stations

Xuchang Tang
Xinfan Lin*
Dept. of Mech. & Aero. Eng.
University of California, Davis
Davis, California, 95616, USA
lxflin@ucdavis.edu

Shuang Feng
Samuel Markolf
Ricardo de Castro
Dept. of Mech. Eng.
University of California, Merced
Merced, California, 95343, USA

Qijian Gan,
Scott Moura
California PATH
University of California, Berkeley
Berkeley, California, 94720, USA

2024 IEEE 27th International Conference on Intelligent Transportation Systems (ITSC) | 979-8-3315-0592-9/24/$31.00 ©2024 IEEE | DOI: 10.1109/ITSC58415.2024.10919547

***Abstract*—Electric vehicles (EVs) pose significant challenges for long-distance mass evacuation during natural hazards due to their long charging time compared to traditional gasoline vehicles. This paper studies the evacuation planning for high EV ownership regions by exploring the optimization of route selection, vehicle grouping, and departure and charging scheduling. More importantly, we also consider the Mobile Charging Stations (MCS), which can be deployed temporarily to supplement the Fixed Charging Stations (FCS) for the evacuation operation, and study the optimization of their placement. The overall optimization scheme is divided into two phases: route optimization via a recursive Dijkstra algorithm and combined vehicle grouping, scheduling, and MCS deployment through constrained Mixed Integer Linear Programming (MILP). Our case study, using a modified Sioux Falls map, reveals that additional MCSs could significantly reduce average evacuation time (nearly 40% reduction for vehicles required charging in the case study), and gives several other interesting insights. For example, the number of charging ports available at charging stations is identified as a critical factor affecting the size distribution of the evacuating vehicle groups. Strategically, the best locations for MCSs are nodes with the highest number of charging visits and network centrality measures. This pioneering study demonstrates the prominent potential of MCS in enabling EV evacuation in high-risk areas, and the proposed optimization scheme provides a tool for governments and agencies to perform evacuation operation planning, optimization, and evaluation.**

***Index Terms*—Electric Vehicle, Emergency Evacuation, Mobile Charging Station**

I. Introduction

The market of electric vehicles (EV) is fast expanding. From 2011 to December 2023, there were more than 4.5 million EV sales in the US, with 40% in California. However, the EV charging infrastructure is falling behind in the US, with a plug-in vehicle to charger ratio of 17, compared to the world average of 7 [1]. In addition, EV has significantly longer charging time compared to the refueling time of the traditional gasoline vehicles. In North America, the chargers are primarily categorized into 3 levels: Level 1 is residential AC charging that provides 5 miles of range per hour; Level 2 is public charging with a rate of 10-20 miles per hour; Level 3 is the DC fast charging that provides 80% charge in about 30 minutes [2], [3]. For comparison, traditional gasoline vehicles typically take less than 10 minutes for a complete refuel. The long charging time and the sparsity of charging station poses a well-known challenge for long-distance travel of EV.

Meanwhile, mass evacuation of community is becoming more frequent due to nature hazards. Wildfires are common in California due to the unique climate pattern. Several wildfires in recent history were widespread to an extent that required massive evacuations. For example, approximately 52,000 residents were evacuated in the Town of Paradise because of the Camp Fire in 2018 [4], and during the Kincade Fire in 2019, the Sonomas County evacuated nearly 200,000 people with a state of emergency declared [5]. Hurricane is another major disaster affecting a wide range of areas and population. For instance, Hurricane Irma in 2017 forced an evacuation of at least 6 million people in the state of Florida, Georgia, and South Carolina [6]. The evacuation caused by Hurrican Irma also relied heavily on personal vehicles. In a study with 170,000 affected individuals, more than 50% of the population who responded to the evacuation order need to travel more than 50 miles [7].

The increasing adoption rate of EVs poses new challenges for the planning and organization of mass evacuation. The goal of evacuation is to make sure that all vehicles (and the affected population) could reach the safe destination in minimal (or at least permissible) time. Evacuation planning needs to find answers to several key questions, including (1) How many vehicles should be placed in each group to be evacuated together? (2) When should each vehicle group depart? (3) Which route should each group take? and (4) Where should vehicles stop for refueling/recharging?

Multiple studies have been conducted on evacuation planning for traditional vehicles. For example, [8] formulated the evacuation planning as a multi-objective problem, and

*Corresponding author
This work is supported by the California Climate Action Seed Grants of the University of California (Grant No.R02CP6996)

solved with a three-step approach, including safe area designation, destination selection, and optimal path finding. A study in 2006 conducted by [9] focused on the journey scheduling between a selected set of origin and destination nodes. This 2006 study formulated the problem in a system-optimal dynamic traffic assignment format with an objective of minimizing network clearance time (longest evacuation time), and solved using an iterative heuristic approach. Another study completed by [10] in 2020 investigated a bus-based evacuation with considerations on external environment uncertainties. The bus-based evacuation study formulated the evacuation planning into three optimization problem, including (1) minimizing the number of buses needed; (2) minimizing the maximum evacuation time; and (3) minimizing the max difference in solutions from (1) and (2).

Recent studies have also investigated evacuation planning for EVs [11]–[15]. Specifically, a 2022 study by [14] considered an EV-only evacuation scenario by formulating a three-stage problem, including consolidating network by pre-assigning charging stations, ranking node significance based on paths, and solving the evacuation planning as a mixed integer linear programming with the objective of minimizing total evacuation time. Another research carried out by [15] in 2022 formulated the evacuation route planning as a minimum spanning tree problem with hop constraints, and minimized the total evacuation time using a branch-and-price heuristic algorithm. The work also conducted numerical experiments to show improved evacuation performance with denser and optimally-sited refueling (charging) infrastructures. The conclusion suggests a potential need for more charging stations in urgent situations.

The contribution of this work is to introduce mobile charging stations (MCS) to address the fundamental challenge facing EV evacuation planning in the state of art. It is important to note that almost all existing works on EV evacuation planning point to the lack of charging stations as a main bottleneck and suggest the need for significant expansion of charging infrastructure. More critically, the distribution of the fixed charging stations (FCS) is spatially uneven and does not adequately serve people from all social backgrounds [16], [17]. The situation is worsening as the rapid growth of EVs is outpacing the construction of FCS [18]. Even if the number of charging stations increases substantially in future, their placement is likel y to be optimized for daily EV usage pattern rather than for the atypical scenarios of mass evacuations, where large number of EVs need to travel on routes they do not usually take.

Mobile charging stations are temporary charging infrastructures that can provide EV charging services at convenient time and locations, such as battery-integrated trucks [19], [20]. They are especially beneficial under mass evacuation scenarios, where there is a sudden surge in spatial and temporal charging need and the power system is fragile.

We propose to formulate a set of multi-layer optimization problems including evacuation route selection, EV grouping, and scheduling of departure and charging time. More importantly, we consider the availability of MCSs, and perform the optimization of their locations together with the evacuation scheduling problem. The eventual goal is to minimize the total evacuation time under the mass EV evacuation setting. To the best of the authors knowledge, this is the first work that integrates MCS into the planning of EV evacuation operation, and we will demonstrate the tremendous potential of MCS in improving evacuation efficiency along with other interesting insights and findings.

II. Overall Problem Statement

An evacuation scenario consists of the following three key aspects: map, evacuation demand, and vehicle parameters.

Our goal for evacuation planning is to minimize the summed evacuation time: given the map of the evacuation area, evacuation demand, vehicle data, and MCS availabilities, we want to determine which routes to take, which and how many vehicles to group together, when to depart, where to charge, what energy level to charge to, and where to place the MCS, such that the summed evacuation time for all vehicles is minimized. The problem is divided into two stages, as shown in Figure 1. Stage 1 focuses on finding feasible routes, and stage 2 focuses on vehicle grouping, vehicle departure scheduling, evacuation route and charging station selections, and MCS placements.

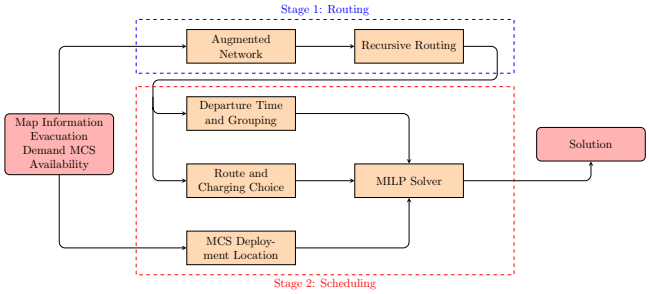

Fig. 1. Two-Stage Approach

We assume no queuing behavior at the charging stations due to the nature of the two-stages process. All vehicles will wait only at their origin if they need to. We further exclude real-time traffic effects as public roads will be prepared under evacuation settings.

III. Stage 1: Evacuation Route Selection

A. Problem Statement

Given a network $G(\mathbb{N}, \mathbb{E})$ with a set of nodes $\mathbb{N}$ and edges $\mathbb{E}$, we want to find the K shortest paths $\{p_0, \cdots, p_{K-1}\}$. A valid path p is defined as a series of nodes that are connected with edges in-between. A complete path must have the first and last nodes as the designated origin and destination nodes. Additionally, vehicles following any path p_i should have a state of charge (SOC) bounded between a certain range $soc_t \in [\underline{soc}, \overline{soc}]$, $\forall t \in \mathbb{T}$, where $\mathbb{T}$ indicates the set of all timestamps. SOC is defined as the ratio of the EV remaining energy level to the battery capacity in percentage.

B. Method

1) Network: In the network G, intersections and locations of interest are modeled as nodes $n \in \mathbb{N}$, and the roads connecting the nodes are modeled as edges $\mathbb{E}$. The connectivity of nodes is represented by an adjacency matrix A, with $A_{i,j} = 1$ indicating the presence of connection from node n_i to node n_j. A network is also associated with cost matrices C. Specifically, three cost matrices are considered: distance C^d, time C^t, and energy costs C^e. The distance cost C^d consists of entries C^d_{ij} indicating the Euclidean distance between nodes n_i and n_j. For time cost C^t, each entry C^t_{ij} indicates the travel time to reach node n_j from node n_i, which is calculated as $C^t_{ij} = \frac{C^d_{ij}}{v_{ij}}$, where v_{ij} is the vehicle velocity from node n_i to n_j. Similarly, the energy cost is calculated as $C^e_{ij} = \frac{C^d_{ij}}{\eta_{ij}}$, where η_{ij} is the energy consumption rate from node i to node j. For all cost matrices, $C_{ij} = \infty$ if $A_{ij} = 0$.

2) Augmented Network with Virtual Nodes: For the EV evacuation problem, charging behavior also needs to be incorporated into the network. We augment the original network by representing charging as travelling on an edge with a negative energy cost (increase in SOC). The charging behavior modelling is illustrated in Figure 2.

Specifically, in the new augmented network $\tilde{G}$, a node is said to have charging capability if it has fixed charging station (FCS) or can accommodate MCS deployment. For each of these nodes n, a series of virtual nodes $\{\tilde{n}_1, \cdots, \tilde{n}_{N_\%}\}$ are appended to it, each or which represents a charging target in SOC. For example, we can have 3 virtual nodes representing charging to 50%, 75%, and 100% respectively. Upon arriving at a charging node, the vehicle has multiple options: either skip charging and continue the route; or charge by "driving" towards one of the virtual nodes, taking positive time cost and negative energy cost. After completion of charging, the vehicle would continue its journey towards the next real node.

In the new network, the augmented adjacency matrix $\tilde{A}$ keeps its upper left portion the same as the original adjacency matrix A. For every physical node n with a charging virtual node n_c, the adjacency matrix $\tilde{A}$ assigns a new connection, $\tilde{A}_{n,n_c} = 1$. Additionally, for each $n^+ \in succ\{n\}$, where $succ\{n\}$ indicates the successor set of node n in the original network, $\tilde{A}_{n_c,n^+} = 1$, allowing vehicles to continue the journey after charging. This augmentation is also applied to cost matrices. For example, new elements $\tilde{C}_{n_c,n^+} = C_{n,n^+}$, and $\tilde{C}_{n,n_c}$ are added to reflect the charging cost.

The augmented network enables the application of well-known path-finding approaches such as the Dijkstra's Algorithm, while admitting charging time and final SOC at each charging station as optimization variables.

3) Routing Algorithm: We propose a routing algorithm based on a modified version of the Dijkstra's Algorithm, which is an efficient method for finding the shortest path in a network.

At any intermediate stage of routing, we define a set $\bar{\mathbb{N}}_v$ containing all previously visited nodes as the visited set. We already know the shortest path to all the nodes in the set from origin upon finishing the preceding optimization. We also define a set $\mathbb{N}_u$ containing all the neighboring nodes of $\bar{\mathbb{N}}_v$, excluding nodes already included in $\bar{\mathbb{N}}_v$ as the unvisited set. The neighbor set of a node n is defined as $\mathbb{N}_n(n) = \{n_n | A_{n,n_n} = 1\}$. We define the minimal accumulated cost from node i to node j as $\hat{c}^i_j$. The algorithm is initialized with $\bar{\mathbb{N}}_v = \{n_o\}$ and $\hat{c}^{n_o}_i = \infty, \forall i \in \mathbb{N} \setminus n_o$, i.e. infinite cost between origin n_o and any node before optimization. At each iteration, for each visited node n in $\bar{\mathbb{N}}_v$ and each neighbor node $n_n \in \mathbb{N}_n(n)$, the algorithm checks whether the path through n offers a smaller cost $\hat{c}^{n_o}_{n_n}$, and updates $\hat{c}^{n_o}_{n_n} = \hat{c}^{n_o}_n + C_{n,n_n}$. After examining the costs to all neighbors, the Dijkstra's algorithm picks the neighbor node with the smallest cost from origin to visit and start the next iteration. The algorithm eventually stops when the selected node to visit is the destination n_d, leaving a set of selected nodes as the shortest path from n_o to n_d. In our application, we use the time cost to determine the shortest path, while also keeping track of the energy costs for the purpose of accommodating the bound on SOC. That is, given an initial SOC at departure soc_{init}, the cost $\hat{c}^{n_o}_j = \infty$ if the SOC after traveling to node j will be outside the bound $[\underline{soc}, \overline{soc}]$. More details about the Dijkstra's algorithm can be found in [21]. Other methods such as A^* can also be used [22], while we will demonstrate with the Dijkstra's Algorithm due to its simplicity.

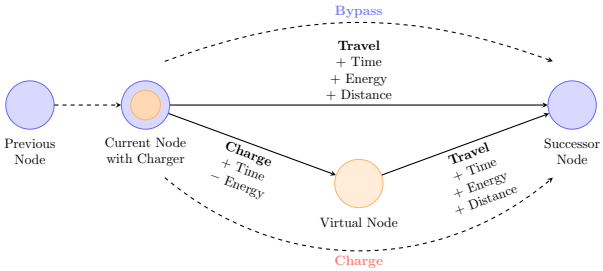

Fig. 2. Using Virtual Nodes to Represent Charging Behavior

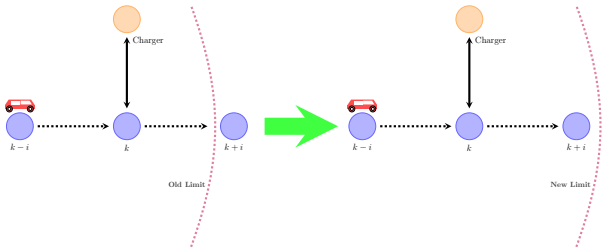

Fig. 3. Dynamic/Non-stationary Network due to Charging at Virtual Nodes

Noted that the Dijkstra's Algorithm can only be applied to a stationary network, but in this application, the network is dynamic due to charging, as illustrated in Fig. 3. Specifically, the initial SOC soc_{init} poses a range limit on the vehicle, disconnecting the outside nodes from inside (cut-off edges). The range limit expands if the vehicle takes a route with charging at virtual nodes, equivalent to re-establishing the connections. The network is hence considered as dynamic

due to the resultant changes in edges and the adjacency matrix.

To overcome the problem of path-finding in a dynamic network, we first observe that change in network only occurs when the vehicle charges. Since charging is modeled as traveling towards a virtual node, the network is static before and after visiting any virtual node. We propose a modified recursive Dijkstra's algorithm to address the dynamic problem. Specifically, whenever the route selection procedure reaches a virtual node, we create a new nested iterative path-finding loop with the same destination, but with the current node as the new origin and the current SOC as the new initial SOC. This new loop will generate a sub-path, and all sub-paths constitute the overall path. Noted that optimal sub-paths, however, do not guarantee the optimality of the combined overall path. To address the potential non-optimality, We apply the modified recursive Dijkstra's algorithm repeatedly to generate a set of K shortest (cost-optimal) paths from the origin to the destination nodes. At each run, we mask all previously appeared combinations of virtual (charging) nodes to enforce exploration of other possible routes. The iteration stops once there is no more unmasked virtual node or when the current path is infeasible. The shortest K paths are then selected from the generated ones, sorted by journey time. In this way, even if we obtain a sub-optimal path at a single run, the true optimal path will still be present in the final selected set of paths. Moreover, multiple paths are usually needed for the subsequent evacuation scheduling problem, as a single path is most likely not sufficient to evacuate all the vehicles timely.

IV. Stage 2: Evacuation Scheduling and MCS Deployment

A. Problem Statement

For each origin-destination (OD) pair $w(n_o, n_d)$ in the full set $\mathbb{W}$, given the set of available paths $\mathbb{P}_w$ between each OD pair w (obtained from routing), the goal is to find the optimal schedule of vehicle departure time and MCS locations such that the summed evacuation time for all evacuees is minimized.

We will use discrete time representation, where the time $t \in \mathbb{T}$ takes discrete non-negative integer values. We formulate the scheduling and MCS deployment problem in a mixed-integer linear programming (MILP) format, which is then solved using Gurobi [23].

B. Decision Variables

1) EV Departure Scheduling: We use integer x_{wpt} to represent the number of EVs evacuated through an origin-destination pair w following a path p and departing at time t.

2) MCS Deployment: We use q_{mnt} to denote the presence of an MCS m at a node n at time t. Specifically, q_{mnt} is binary, $q_{mnt} \in \{0, 1\}$, with 1 indicating deployment/presence, and 0 representing absence.

C. Objective

The objective is the summed evacuation time of all vehicles,

$$\sum_{w\in\mathbb{W}} \sum_{p\in\mathbb{P}_w} \sum_{t\in\mathbb{T}} (t + \tilde{t}_{wpt}) \times x_{wpt}, \tag{1}$$

where $\tilde{t}_{wpt}$ denotes the total travel and charging time for any vehicle evacuated between origin-destination pair w following path p and departing at time t. This can be pre-calculated from the routing stage.

D. Auxiliary Variables

1) Charging Port Supply:

$$S_{nt} = S_{fcs,n} + s_{mcs} \times \sum_{m\in\mathbb{M}} q_{mnt}, \forall n \in \mathbb{N}, \forall t \in \mathbb{T}, \tag{2}$$

where $S_{fcs,n}$ is the existing number of fixed charging ports at node n, and s_{mcs} is the number of ports per MCS.

2) Charging Port Demand:

$$D_{nt} = \sum_{w\in\mathbb{W}} \sum_{p\in\mathbb{P}_w} \sum_{\tau\in\mathbb{T}} (x_{wp\tau} \times h_{wp\tau nt}), \forall n \in \mathbb{N}, \forall t \in \mathbb{T} \tag{3}$$

where $h_{wp\tau vt} \in \{0, 1\}$ is the charging indicator, with 1 indicating that the vehicle traveling between origin-destination pair w following path p and departing at time τ will charge at node n at time t.

3) MCS Port Demand:

$$D_{mcs,nt} = max(D_{nt} - S_{fcs,n}, 0), \forall n \in \mathbb{N}, \forall t \in \mathbb{T} \tag{4}$$

When the total charging demand D_{nt} exceeds the FCS supply $S_{fcs,n}$, the deficit is the demand for MCS $D_{mcs,nt}$. Otherwise, the demand for MCS is 0. Note that this constraint is nonlinear but can be linearized.

4) MCS Energy Demand:

$$E_{nt} = r_c \times \sum_{\tau=0}^{t} D_{mcs,n\tau}, \forall n \in \mathbb{N}, \forall t \in \mathbb{T}, \tag{5}$$

which is the accumulated charging port demands on MCS $D_{mcs,nt}$ multiplied by the charging rate r_c.

5) MCS State of Charge:

$$soc_{mt} = 1 - q_{mnt} \frac{E_{nt}}{e_{mcs} \sum_{n\in\mathbb{N}} q_{mnt}}, \forall m \in \mathbb{M}, \forall t \in \mathbb{T}, \tag{6}$$

which represents the remaining energy level of each MCS in percentage, and e_{mcs} is the energy capacity of a single MCS.

E. Constraints

1) Evacuation Demand:

$$\sum_{p\in\mathbb{P}_w} \sum_{t\in\mathbb{T}} x_{wpt} = f_w, \forall w \in \mathbb{W} \tag{7}$$

All the vehicles need to be evacuated, where f_w is the total number of vehicles assigned to each OD pair w.

2) Single-site MCS Deployment:

$$\sum_{n\in\mathbb{N}} |q_{mnt}| = 1, \forall m \in \mathbb{M}, \forall t \in \mathbb{T} \tag{8}$$

Each MCS cannot be placed at more than one node at any given time. Note that this constraint is nonlinear but can be linearized as well.

3) Port Limit:

$$D_{nt} \leq S_{nt}, \forall n \in \mathbb{N}, \forall t \in \mathbb{T} \tag{9}$$

The charging demand at any time cannot exceed the supply of charging ports.

4) MCS Energy:

$$0 \leq soc_{mt} \leq 1, \forall m \in \mathbb{M}, \forall t \in \mathbb{T} \tag{10}$$

The MCS SOC needs to be bounded between 0% and 100%.

V. Case Study

For case study, we selected a modified map of Sioux Falls, which is based on the geography of the region but with extended range. The map has been frequently used for similar studies [15], [24]. The abstracted network is shown in Figure 4.

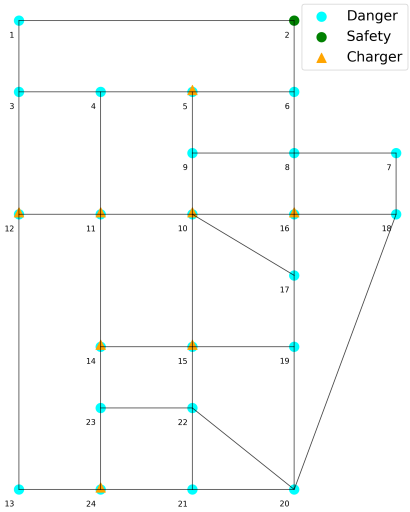

Fig. 4. Sioux Falls Network

We assume each FCS has 50 charging ports, with some nodes having multiple FCSs. The evacuation demand (# of EVs to evacuate) and the number of existing fixed charging ports at each node are listed in Table I. We consider a hypothetical disaster affecting all nodes except node 2, and evacuation starts at 4am on June 23. Thus, all nodes have a positive evacuation demand except node 2, which is the destination/shelter node n_d. There are a total of $35,660$ vehicles registered for evacuation, and a total of 800 ports from existing FCSs. The longitudinal (East-West) range is 370 km, and the latitudinal (North-South) range is 460 km. The longest evacuation distance is 730 km from node 13 to node 2.

Each MCS is considered to have 20 ports and an energy capacity of $420\ kWh$. We restrict the MCSs to be deployed at nodes with existing FCS because of the space availability, and there is no upper limit on the number of MCSs deployable at any node. Each MCS is pre-deployed at the designated site and stay throughout the entire evacuation period. We allow a vehicle to either bypass charging or charge to 100% SOC when passing a charging node, i.e. 1 virtual node for each physical node. In the first 3 subsections of this case study, we assume that all vehicles have the same parameters, including the battery size of $57.5\ kWh$ (or a range of $362\ km$), traveling speed of 80 $\frac{km}{h}$, energy consumption rate of 6.3 $\frac{km}{kWh}$, and initial SOC of 100%. In the last subsection, we demonstrate the feasibility of our method in handling distributed vehicle parameters (initial SOCs) with group size limit (considering road capacity) in more realistic scenarios. All these assumptions/restrictions can be easily relaxed (ongoing in current work), as the purpose of this paper is to demonstrate the feasibility and capability of the proposed method. The proposed evacuation planning scheme is implemented and run on the case study map under a range of available number of MCSs. The results are discussed as follows.

TABLE I
Evacuation Demand and FCS Ports Allocation

Node Label	# EVs to evacuate	FCS Ports	Node Label	# EVs to evacuate	FCS Ports
1	880	-	13	1460	-
2	0	-	14	1410	200
3	280	-	15	2140	150
4	1160	-	16	2610	50
5	610	50	17	2340	-
6	760	-	18	480	-
7	1210	-	19	1280	-
8	1670	-	20	1850	-
9	1620	-	21	1100	-
10	4520	150	22	2440	-
11	2230	50	23	1450	-
12	1390	50	24	770	100

A. Evacuation Time Reduction enabled by MCS

The effect of number of available MCSs on the average evacuation time is shown in Figure 5. Recall that the evacuation time of a vehicle is defined as the elapsed time from the beginning of evacuation to the vehicle arrival time at destination, and the summed evacuation time is the objective of optimization formulated in Eqn. (1). Since some vehicles do not require charging (due to its proximity to the destination), both the average evacuation time of all vehicles and that of those need charging are shown in the figure. In addition, the shaded area represents the 25% and 75% quantile of the evacuation time distribution.

Figure 5 shows the significant reduction in average evacuation time by introducing MCS. Specifically, compared to the baseline case (no MCS), with just 5 MCSs, we observe a reduction of 75 minutes (11%) in average evacuation time for all vehicles, and a reduction of 164 minutes (14%) for all vehicles that requires charging. As the number of MCSs increases to 40, the reduction in evacuation time is found to be 200 minutes (30%) for all vehicles, and 445 minutes (38%) for vehicles requiring charging. Additionally, the quantile bound also decreases as more MCSs are introduced. The narrower bound indicates a more concentrated distribution of the evacuation time among vehicles, and hence the more timely evacuation of the overall vehicle population.

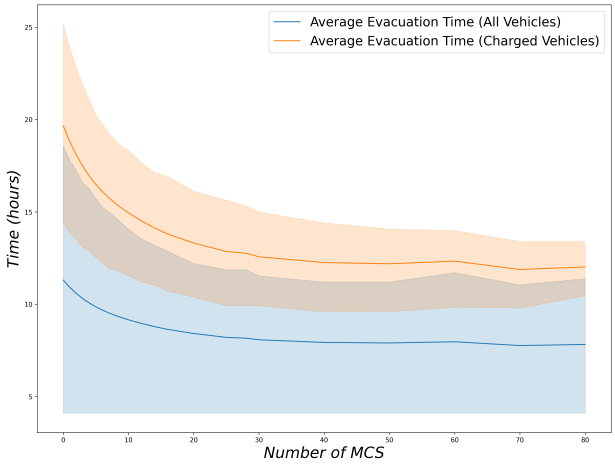

Fig. 5. Evacuation Time under Different Numbers of MCSs

B. Optimal Scheduling Pattern

We then demonstrate and analyze the patterns of the optimized vehicle departure schedule. Figure 6 shows an example Gantt chart for the grouped vehicle evacuation with 1 MCS, where each line shows the start and end time of a vehicle group. For example, the third line indicates that there is a group of 30 EVs departing at 5am and arriving at roughly 10:30am. The departure schedule are determined by the aforementioned decision variable x_{wpt}, which governs the number of vehicles that should depart at time t following path p.

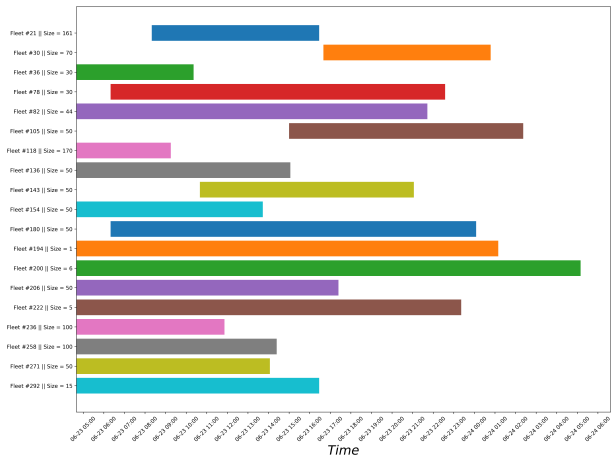

Fig. 6. Gantt Chart of Vehicle Evacuation Schedule with 1 MCS

From the results, it is interesting to notice certain patterns of the optimal schedule, such as the distribution of the vehicle group size. Figure 7 shows the histogram of the sizes of groups charged at least once for the case of 1 MCS. An obvious correlation can be observed between the group size and the number of charging ports. Specifically, the group size with the highest occurrence is 50, which accounts for 46% of the groups. This is actually the number of ports for a unit FCS. There are other peaks at 20, 70, 100, 120, which are either multiples of FCS ports, MCS ports, or the sum of them, denoted by the the green, red, and orange ticks in Figure 7. The correlation of peaks with the port numbers suggests that the optimal scheduling behavior is to maximize the occupancy of ports. Intuitively, when assigning certain vehicle groups to the charging node, a solution that maximizes the port usage by matching the group size to the number of available ports is superior to any solution that does otherwise, under the objective of minimizing the summed evacuation time. In other words, the number of ports is a limiting factor of vehicle group size (at least in this case study).

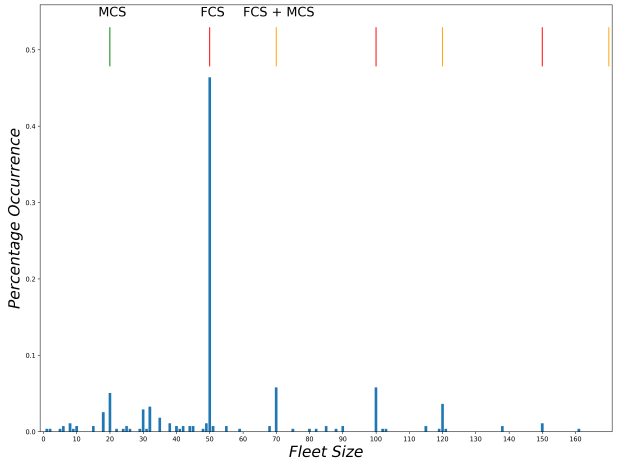

Fig. 7. Distribution of Vehicle Group Size under 1 MCS

C. MCS Deployment Pattern

We further investigate the MCS deployment pattern by inspecting their locations under different number of total available MCSs. It is interesting to note that (at least) in a range of total MCS numbers, specifically 1-50 in our case study, all MCSs are placed at a single node, i.e. node 10. This pattern can be explained by the centrality of nodes and charging traffic distribution.

The centrality of a node in a network can be quantified by different measures. For example, degree centrality is a measure based on the number of neighbors a node has. Betweenness centrality counts the number of shortest paths between all node pairs that pass through the node. Eigenvector centrality uses the eigenvalue decomposition of the adjacency matrix A to measure the level of influence of a node in the network. Figure 8 shows the normalized degree, betweenness, and eigenvector centrality measures of all the nodes. We notice that node 10 has the highest centrality in all three measures, marked by the golden star in the figure.

We have also analyzed the distribution of the charging activities among charging nodes. Figure 9 shows an example case with 10 MCSs. The blue bars indicate the vehicle charging visits of each node as a percentage of the total charging activities in the baseline case with no MCS, and the orange bars indicate those with 10 MCSs. Noted that the distribution of vehicle charging visits indicates the dominance of node 10. In fact, in the baseline case, node 10 accounts

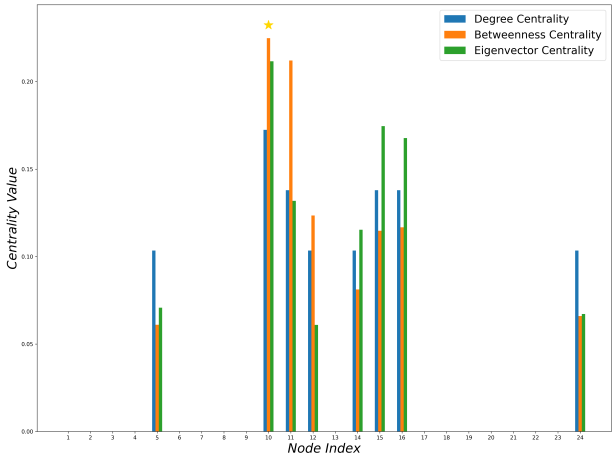

Fig. 8. Normalized Charging Node Centrality Measures

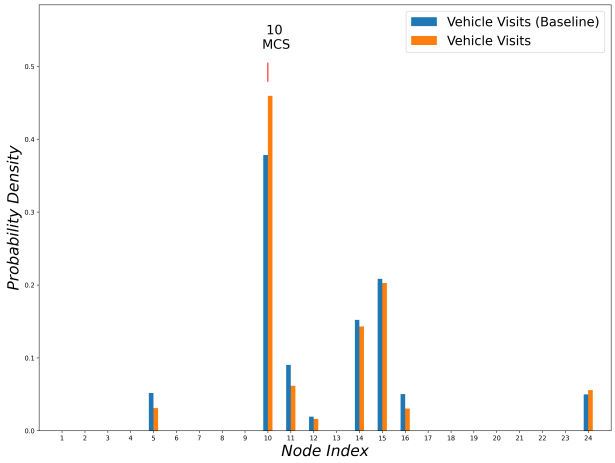

Fig. 9. Charging Visits Frequencies and MCS Location with 10 MCS

for around 40% of the total charging activities (visits), almost twice as the secondary peak at node 15. The dominance is more prominent with 10 MCSs deployed.

Therefore, due to the high centrality of node 10 in the network, paths through node 10 are among the shortest for evacuation between different OD pairs. Consequently, in order to achieve the minimum total evacuation time, the optimal departure and charging strategy will schedule a large amount of charging visits at node 10 in the baseline case (with no MCS), around 40% in the case study, while the remaining 7 charging nodes only account for 60% (around 8% each). Then, when deploying the MCS, it is intuitive to have most or all of the MCSs deployed at the dominant node 10, so that more vehicles could take the shortest evacuation path to reduce the evacuation time most effectively.

D. Extended Studies Considering Initial EV Energy Distribution and Traffic Constraints

To show the feasibility of our proposed method in accommodating more realistic real-world evacuation scenarios, we conducted another case study with two major modifications in the setting. First, we impose a 850 upper limit on the EV group size considering the traffic capacity to avoid congestion. The cap is an estimate based on the two-lane highway capacity of $3,400$ vehicles per hour [25] and our operation time step of 15 minutes. Second, we consider variability in EV initial SOCs. Specifically, the initial SOCs are randomly sampled from a uniform distribution over the set $[70\%, 90\%, 100\%]$. We will compare the results with the benchmark case of fixed initial SOC at 100% for all vehicles. All vehicles are equipped with 82 kwh batteries with a range of 517 km, but this assumption can also be relaxed in the similar way by considering a distribution of battery sizes.

The average evacuation time under different numbers of MCSs for the cases of fixed and distributed initial SOCs is shown in Figure 10. A clear increase in evacuation time

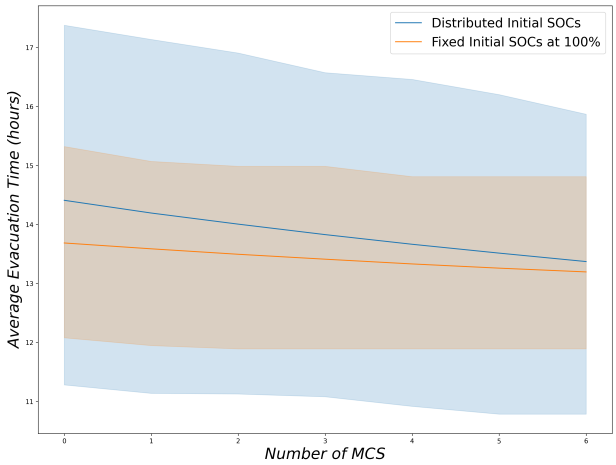

Fig. 10. Evacuation Time Comparison between Fixed and Distributed Initial SOCs for Charged Vehicles under Different Numbers of MCSs

can be observed for the latter case, along with much wider quantile bounds. These results indicate less timely evacuation and high disparity in evacuation time among vehicles, which are caused by the presence of vehicles with departure SOCs lower than 100%. Interestingly, as the number of MCS increases, the difference between the two cases reduces, showing that MCS is even more effective in accelerating the evacuation process for cases with varying (lower) departure SOCs.

Figure 11 shows the group size distribution for both the fixed and distributed initial SOC cases under 1 MCS. The patterns of distribution in the case with fixed 100% initial SOC are similar to those seen in Section V-B, showing a strong correlation with the number of charging ports available at the charging stations. For the case with distributed initial SOCs, the group size distribution is much more spread-out and flat. Specifically, the occurrence of EV groups with the size of 50, which is the number of ports a single FCS can supply, now only accounts for around 18% of the total, compared to 36% in the case with fixed 100% initial SOCs. Other peaks at the multiples of FCS/MCS charging ports are also suppressed, and there are many more smaller group sizes of significant occurrences showing up. This phenomenon can be explained by the fact that various departure SOCs create

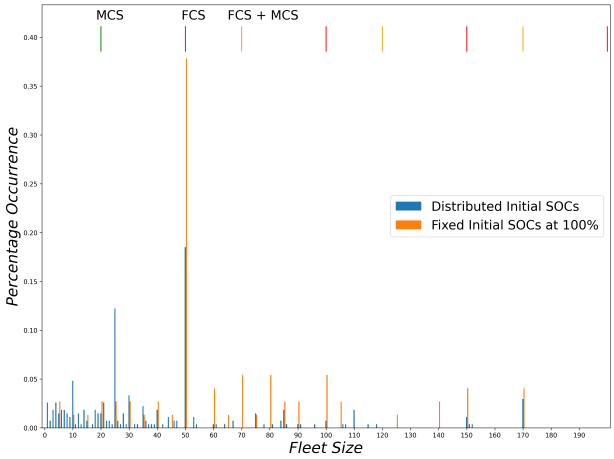

Fig. 11. Distribution of Vehicle Group Sizes in the Fixed and Distributed Initial SOC Cases with 1 MCS

different evacuation demands and add to the complexity of optimization, and hence the optimal scheduling needs to break the EV population into smaller groups in order to generate the departure and charging schedule to accommodate all of them.

VI. Conclusion

In this work, we studied the EV evacuation planning with the introduction of mobile charging stations (MCSs), and demonstrated on a modified Sioux Falls map for case study. Several interesting insights have been obtained from the study. First, with an increasing number of MCSs, we observed significant reduction in average evacuation time (nearly 40% reduction for vehicles requiring charging in the case study), as well as more concentrated distribution of the evacuation time. The reduction in time testifies the significant potential of mobile charging stations in facilitating evacuation operation. Second, the optimal departure schedule organized vehicles into groups, and the distribution of group sizes is highly correlated with the number of charging ports (from FCS and/or MCS). The correlation indicates that the available charging ports at the charging nodes could give insight on the optimal vehicle grouping strategy. Finally, the optimal MCS placement strategy, for the case study, is found to deploy all MCSs at a single node. This interesting pattern can be explained by the highest centrality measure and the dominant charging activities at the node, which provides a simple yet effective heuristic for MCS deployment on such maps. In future works, we will extend the studies by relaxing assumptions. For example, we will allow arbitrary MCS placement at any nodes and MCS recharging and redeployment, as well as consider more diverse distribution of EV initial SOC, battery sizes (ranges), power grid constraints and real-time traffic flow conditions.

References

[1] S. Á. Funke, F. Sprei, T. Gnann, and P. Plötz, "How much charging infrastructure do electric vehicles need? a review of the evidence and international comparison," *Transportation research part D: transport and environment*, vol. 77, pp. 224–242, 2019.

[2] M. S. Mastoi, S. Zhuang, H. M. Munir, M. Haris, M. Hassan, M. Usman, S. S. H. Bukhari, and J.-S. Ro, "An in-depth analysis of electric vehicle charging station infrastructure, policy implications, and future trends," *Energy Reports*, vol. 8, pp. 11504–11529, 2022.

[3] S. Hardman, A. Jenn, G. Tal, J. Axsen, G. Beard, N. Daina, E. Figenbaum, N. Jakobsson, P. Jochem, N. Kinnear, *et al.*, "A review of consumer preferences of and interactions with electric vehicle charging infrastructure," *Transportation Research Part D: Transport and Environment*, vol. 62, pp. 508–523, 2018.

[4] A. Maranghides, W. E. Mell, S. Hawks, M. Wilson, W. Brewer, E. Link, C. Brown, C. Murrill, and E. Ashley, *Camp Fire Preliminary Reconnaissance*. US Department of Commerce, National Institute of Standards and Technology, 2020.

[5] S. D. Wong, J. C. Broader, and S. A. Shaheen, "Review of california wildfire evacuations from 2017 to 2019," tech. rep., University of California, Institute of Transportation Studies, 2020.

[6] S. Wong, S. Shaheen, and J. Walker, "Understanding evacuee behavior: A case study of hurricane irma (2018)," tech. rep., Institude of Transporation Studies at University of California, Berkeley, 2018.

[7] H. Younes, A. Darzi, and L. Zhang, "How effective are evacuation orders? an analysis of decision making among vulnerable populations in florida during hurricane irma," *Travel behaviour and society*, vol. 25, pp. 144–152, 2021.

[8] M. Saadatseresht, A. Mansourian, and M. Taleai, "Evacuation planning using multiobjective evolutionary optimization approach," *European journal of operational research*, vol. 198, no. 1, pp. 305–314, 2009.

[9] H. Sbayti and H. S. Mahmassani, "Optimal scheduling of evacuation operations," *Transportation Research Record*, vol. 1964, no. 1, pp. 238–246, 2006.

[10] N. B. Bolia *et al.*, "Robust scheduling for large scale evacuation planning," *Socio-Economic Planning Sciences*, vol. 71, p. 100756, 2020.

[11] K. Feng, N. Lin, S. Xian, and M. V. Chester, "Can we evacuate from hurricanes with electric vehicles?," *Transportation research part D: transport and environment*, vol. 86, p. 102458, 2020.

[12] L. Lu, *Designing electric vehicle charging infrastructure to enable disaster evacuation*. PhD thesis, 2022.

[13] J. Zhang and X. Zhang, "A multi-trip electric bus routing model considering equity during short-notice evacuations," *Transportation Research Part D: Transport and Environment*, vol. 110, p. 103397, 2022.

[14] Q. Li, S. Soleimaniamiri, and X. Li, "Optimal mass evacuation planning for electric vehicles before natural disasters," *Transportation research part D: transport and environment*, vol. 107, p. 103292, 2022.

[15] D. S. D. Purba, E. Kontou, and C. Vogiatzis, "Evacuation route planning for alternative fuel vehicles," *Transportation research part C: emerging technologies*, vol. 143, p. 103837, 2022.

[16] M. Nicholas, D. Hall, and N. Lutsey, "Quantifying the electric vehicle charging infrastructure gap across us markets," *Int. Counc. Clean Transp*, vol. 20, pp. 1–39, 2019.

[17] M. Nazari-Heris, A. Loni, S. Asadi, and B. Mohammadi-ivatloo, "Toward social equity access and mobile charging stations for electric vehicles: A case study in los angeles," *Applied Energy*, vol. 311, p. 118704, 2022.

[18] T. Nogueira, E. Sousa, and G. R. Alves, "Electric vehicles growth until 2030: Impact on the distribution network power," *Energy Reports*, vol. 8, pp. 145–152, 2022.

[19] S. Afshar, P. Macedo, F. Mohamed, and V. Disfani, "Mobile charging stations for electric vehicles—a review," *Renewable and Sustainable Energy Reviews*, vol. 152, p. 111654, 2021.

[20] Y. Zhang, X. Liu, W. Wei, T. Peng, G. Hong, and C. Meng, "Mobile charging: A novel charging system for electric vehicles in urban areas," *Applied Energy*, vol. 278, p. 115648, 2020.

[21] E. W. Dijkstra, "A note on two problems in connexion with graphs," in *Edsger Wybe Dijkstra: his life, work, and legacy*, pp. 287–290, 2022.

[22] P. E. Hart, N. J. Nilsson, and B. Raphael, "A formal basis for the heuristic determination of minimum cost paths," *IEEE transactions on Systems Science and Cybernetics*, vol. 4, no. 2, pp. 100–107, 1968.

[23] "Gurobi optimizer reference manual."

[24] X. Sun, Z. Chen, and Y. Yin, "Integrated planning of static and dynamic charging infrastructure for electric vehicles," *Transportation Research Part D: Transport and Environment*, vol. 83, p. 102331, 2020.

[25] W. Reilly, "Highway capacity manual 2000," *Tr News*, no. 193, 1997.